STAB'97, Six International Conference on Stability of Ships and Ocean Structures, Pages 137-150, Varna, Bulgaria, September 22-27, 1997.

Reprinted: 08-10-2000
Website: www.shipmotions.nl

Report 1092-P, September 1997,
Delft University of Technology,
Ship Hydromechanics Laboratory,
Mekelweg 2, 2628 CD Delft,
The Netherlands.

Liquid Cargo and Its Effect on Ship Motions

J.M.J. Journée
Delft University of Technology

Summary

When a double bottom tank, a cargo tank or a space in a rolling vessel contains a fluid, gravity waves will appear at the surface of this fluid. These gravity waves will cause exciting roll moments on the vessel. At lower water depths, resonance frequencies can be obtained with high wave amplitudes. A hydraulic jump or bore, which is a strongly non-linear phenomenon, travels periodically back and forth between the walls of the tank. A theory, based on gasdynamics for the shock wave in a gas flow, has been used to describe the motions of the fluid. At higher water depths, the behaviour of the fluid tends to be more linear. Then, a linear potential theory, as used in strip theory ship motions computer programs, is used to describe the motions of the fluid in the tank.
Available experimental data on the behaviour of the fluid in free surface anti-rolling tanks have been used to verify the theoretical approaches for low water depths.
Also, forced roll oscillation tests were carried out with a 2-D model a cargo tank of an LNG carrier for a wide range of filling levels. These experimental data have been used to verify the theoretical results for all water depths.
Finally, a ship model was equipped with liquid cargo tanks and it has been tested in beam waves at zero forward speed. The measured roll data of the model have been compared with the results of strip theory calculations.
It has been concluded that the approaches given in this paper, based on theories developped already in the sixties, can be used to include the effect of non-viscous liquid cargo in ship motions calculations.

1 Introduction

When a tank that contains a fluid with a free surface is forced to carry out roll oscillations, resonance frequencies can be obtained with high wave amplitudes at lower water depths. Under these circumstances a hydraulic jump or bore is formed, which travels periodically back and forth between the walls of the tank. This hydraulic jump can be a strongly non-linear phenomenon. A theory, based on gas-dynamics for the shock wave in a gas flow under similar resonance circumstances, as given by Verhagen and van Wijngaarden (1965), has been adapted and used to describe the motions of the fluid. For low and high frequencies and the frequencies near to the natural frequency, different approaches have been used. A calculation routine has been made to connect these regions. Available

experimental data on the behaviour of the fluid in free surface anti-rolling tanks, obtained from van den Bosch and Vugts, have been used to verify this approach.
At higher waterdepths, the behaviour of the fluid tends to be more linear. Then, the linear potential theory with the pulsating source method of Frank (1967), as used in strip theory ship motions computer programs, has been used to describe the motions of the fluid in the tank. Forced roll oscillation tests were carried out with a 2-D model of a cargo tank of an LNG carrier, to measure the exciting moments for a wide range of filling levels and frequencies and to compare these with theoretical predictions.
Finally, a ship model was equipped with three of these liquid cargo tanks and tested in beam waves at zero forward speed. Several filling levels and two regular wave amplitudes were used to investigate the effect on the roll behaviour of the ship. The measured data have been compared with the results of 2-D potential calculations.

2 LIQUID CARGO LOADS

Observe a rectangular tank with a length l and a breadth b, which has been filled until a water level h with a fluid with a mass density r. The distance of the bottom of the tank above the center of gravity of the vessel is s.

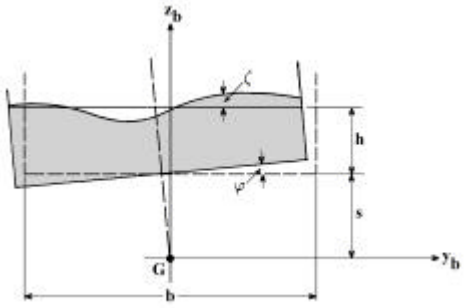

Figure 1 Axis system and Notations

Figure 1 shows a 2-D sketch of this tank with the axis system and notations.

The natural frequency of the surface waves in a harmonic rolling tank appears as the wavelength l equals twice the breadth b, so: $l_0 = 2 \cdot b$.
With the wave number and the dispersion relation:

$$k = \frac{2p}{l} \text{ and } w = \sqrt{\frac{p \cdot g}{b} \cdot \tanh\left(\frac{p \cdot h}{b}\right)}$$

it follows for the natural frequency of surface waves in the tank:

$$w_0 = \sqrt{\frac{p \cdot g}{b} \cdot \tanh\left(\frac{p \cdot h}{b}\right)}$$

2.1 Theory of Verhagen et.al.

Verhagen and van Wijngaarden (1965) have investigated the shallow water wave loads in a rolling rectangular container, with the center of rotation at the bottom of the container. Their expressions for the internal wave loads are rewritten and modified in this paper to be useful for any arbitrary vertical position of the center of rotation. For low and high frequencies and the frequencies near to the natural frequency, different approaches have been used. A calculation routine has been made to connect these regions.

Low and High Frequencies

The harmonic roll motion of the tank is defined by:

$$f = f_a \cdot \sin(wt)$$

In the axis-system of Figure 1 and after linearisation, the vertical displacement of the tank bottom is described by:

$$z = z + y \cdot f$$

and after linearisation, the surface elevation of the fluid is described by:

$$z = s + h + z$$

Relative to the bottom of the tank, the linearised surface elevation of the fluid is described by:

$$x = h + z - y \cdot f$$

Using the shallow water theory, the continuity and momentum equations are:

$$\frac{\partial x}{\partial t} + v \cdot \frac{\partial x}{\partial y} + x \cdot \frac{\partial v}{\partial y} = 0$$

$$\frac{\partial v}{\partial t} + v \cdot \frac{\partial v}{\partial y} + g \cdot \frac{\partial x}{\partial y} + g \cdot f = 0$$

In these formulations, v denotes the velocity of the fluid in the y-direction and the vertical pressure distribution is assumed to be hydrostatic. Therefore, the acceleration in the z-direction, introduced by the excitation, must be small with respect to the acceleration of gravity g, so:

$$f_a \cdot w^2 \cdot b << g$$

The boundary conditions for v are determined by the velocity produced in the horizontal direction by the excitation. Between the surface of the fluid and the bottom of the tank, the velocity of the fluid v varies between v_s and $v_s / \cos kh$ with a mean velocity: v_s / kh. However, in very shallow water v does not vary between the bottom and the surface. When taking the value at the surface, it is required that:

$$v = -(s+h) \cdot \dot{f} \quad \text{at} \quad y = \pm \frac{b}{2}$$

For small values of f_a, the continuity equation and the momentum equation can be given in a linearised form:

$$\frac{\partial x}{\partial t} + h \cdot \frac{\partial v}{\partial y} = 0$$

$$\frac{\partial v}{\partial t} + g \cdot \frac{\partial x}{\partial y} + g \cdot f = 0$$

The solution of the surface elevation x in these equations, satisfying the boundary values for v, is:

$$x = h - \frac{b \cdot w_0 \left\{ 1 + \frac{(s+h) \cdot w^2}{g} \right\}}{p \cdot w \cdot \cos\left(\frac{p \cdot w}{b \cdot w_0} \right)} \cdot$$

$$\cdot \sin\left(\frac{p \cdot w \cdot y}{b \cdot w_0} \right) \cdot f$$

Now, the roll moment follows from the quasi-static moment of the mass of the frozen liquid $r \cdot l \cdot b \cdot h$ and an integration of x over the breadth of the tank:

$$M_f = r \cdot g \cdot l \cdot b \cdot h \cdot \left(s + \frac{h}{2} \right) \cdot f$$

$$+ r \cdot g \cdot l \int_{-b/2}^{+b/2} x \cdot y \cdot dy$$

This delivers the roll moment amplitude for low and high frequencies at small water depths:

$$M_{af} = r \cdot g \cdot l \cdot b \cdot h \cdot \left(s + \frac{h}{2} \right) \cdot f$$

$$+ r \cdot g \cdot l \cdot b^3 \cdot \left\{ 1 + \frac{(s+h) \cdot w^2}{g} \right\} \cdot$$

$$\cdot \left\{ 2 \left(\frac{w_0}{pw} \right)^3 \tan\left(\frac{pw}{2w_0} \right) - \left(\frac{w_0}{pw} \right)^2 \right\} \cdot f_a$$

For very low frequencies, so for the limit value $w \to 0$, this will result into the static moment:

$$M_f = r \cdot g \cdot l \cdot \left\{ b \cdot h \cdot \left(s + \frac{h}{2} \right) + \frac{b^3}{12} \right\} \cdot f$$

The phase lags between the roll moments and the roll motions have not been obtained here. However, they can be set to zero for low frequencies and to $-p$ for high frequencies:

$$e_{M_f f} = 0 \quad \text{for: } w << w_0$$

$$e_{M_f f} = -p \quad \text{for: } w >> w_0$$

Natural Frequency Region

For frequencies near to the natural frequency w_0, the expression for the surface elevation of the fluid x goes to infinity. Experiments showed the appearance of a hydraulic jump or a bore at these frequencies. Obviously, then the linearised equations are not valid anymore. Verhagen and van Wijngaarden solved the problem by using the approach in gas dynamics when a column of gas is oscillated at small amplitude, e.g. by a piston. At frequencies near to the natural frequency at small water depths, they found a roll moment amplitude, defined by:

$$M_{af} = r \cdot g \cdot \frac{l \cdot b^3}{12} \cdot \left(\frac{4}{p}\right)^4 \cdot \sqrt{\frac{2 \cdot f_a \cdot h}{3 \cdot b}} \cdot \left\{1 - \frac{p^2 \cdot b \cdot (w - w_0)^2}{32 \cdot g \cdot f_a}\right\}$$

The phase lags between the roll moment and the roll motion at small water depths are given by:

$$e_{M_f f} = -\frac{p}{2} + a \quad \text{for: } w < w_0$$

$$e_{M_f f} = -\frac{p}{2} - a \quad \text{for: } w > w_0$$

with:

$$a = 2 \cdot \arcsin\left\{\sqrt{\frac{p^2 b (w - w_0)^2}{24 g f_a}}\right\} - \arcsin\left\{\sqrt{\frac{p\ b (w - w_0)^2}{96 g f_a - 3p^2 b (w - w_0)^2}}\right\}$$

Because that the arguments of the square roots in the expression for $e_{M_f f}$ have to be positive, the limits for the frequency w are at least:

$$w_0 - \sqrt{\frac{24 g f_a}{b p^2}} < w < w_0 + \sqrt{\frac{24 g f_a}{b p^2}}$$

2.2 Theory of Frank

For the calculation of the 2-D potential mass and damping of ship-like cross sections, Frank (1967) considered a cylinder, whose cross section is a simply connected region, which is fully or partly immersed, horizontally in a previously undisturbed fluid of infinite depth.

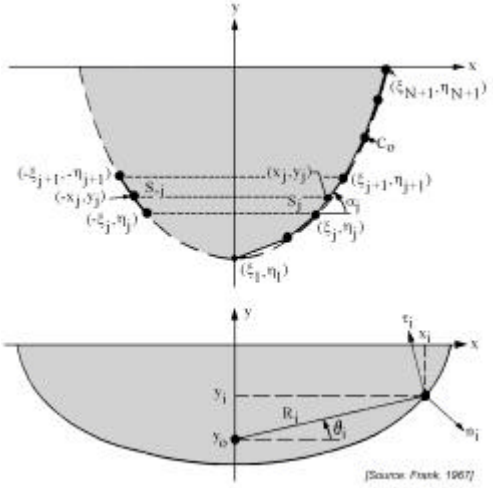

Figure 2 Frank's Axes System

The cylinder, as given in Figure 2, is forced into simple harmonic motion with radian frequency w, according to the displacement equation:

$$S^{(m)} = A^{(m)} \cdot \cos wt$$

The superscript m may take on the values 2, 3 and 4, denoting sway, heave and roll motions, respectively. The roll motions are about an axis through a point $(0, y_0)$ in the symmetry plane of the cylinder.

It is assumed that steady state conditions have been attained. The fluid is assumed to be incompressible, inviscid and irrotational, without any effects of surface tension. The motion amplitudes and velocities are small enough, so that all but the linear terms of the free surface condition, the kinematic boundary condition on the cylinder and the Bernoulli equation may be neglected.

A velocity potential has to be found:

$$\Phi^{(m)} = \mathrm{Re}\left\{f^{(m)}(x, y) \cdot e^{-iwt}\right\}$$

satisfying the equation of Laplace, the symmetry (heave) or anti-symmetry (sway

and roll) condition, the free surface condition, the bottom condition, the kinematic boundary condition at the cylindrical surface and the radiation condition.

Frank has given a potential function, based on pulsating sources and satisfying the boundary conditions. Using earlier work of Wehausen and Laitone, he defined the complex potential at z of a pulsating point source of unit strength at the point z in the lower half plane, as given in Figure 2.

Take the x-axis to be coincident with the undisturbed free surface. Let the cross sectional contour C_0 of the submerged portion of the cylinder be in the lower half plane and the y-axis, positive upwards, being the axis of symmetry of C_0. Select $N+1$ points (x_i, h_i) of C_0 to lie in the fourth quadrant. Connect these $N+1$ points by successive straight lines. Then, N straight-line segments are obtained which, together with their reflected images in the third quadrant, yield an approximation to the given contour as shown in Figure 2.

The coordinates, length and angle associated with the j^{th} segment are identified by the subscript j, whereas the corresponding quantities for the reflected image in the third quadrant are denoted by the subscript $-j$, so that by symmetry $x_{-j} = x_j$ and $h_{-j} = -h_j$ for $1 \le j \le N+1$.

Potentials and pressures are to be evaluated at the midpoint of each segment and for $1 \le i \le N$ the coordinates of the midpoint of the i^{th} segment are:

$$x_i = \frac{x_i + x_{i+1}}{2} \text{ and } y_i = \frac{p_i + h_{i+1}}{2}$$

In the translational modes, any point on the cylinder moves with the velocity:

$$v^{(2)} = -iA^{(2)}w \cdot \sin wt \text{ for sway}$$
$$v^{(3)} = -iA^{(3)}w \cdot \sin wt \text{ for heave}$$

The length of the i^{th} segment and the angle made by this segment with the positive x-axis are:

$$s_i = \sqrt{(x_{i+1} - x_i)^2 + (h_{i+1} - h_i)^2}$$
$$a_i = \arctan\left\{\frac{h_{i+1} - h_i}{x_{i+1} - x_i}\right\}$$

In here a_i is defined as $-p/2 \le a_i \le +p/2$.

If the denominator is negative, depending on the sign of the numerator, p has to be added or subtracted, so that a_i will be defined as $-p \le a_i \le +p$.

The outgoing unit vector normal to the cross section at the i^{th} midpoint (x_i, y_i) is:

$$n_i = +\bar{i} \cdot \sin a_i - \bar{j} \cdot \cos a_i$$

where $\bar{i}$ and $\bar{j}$ are unit vectors in the directions x and y, respectively.

The roll motion is illustrated in Figure 2 and considering a point (x_i, y_i) on C_0, an inspection of this figure yields:

$$R_i = \sqrt{x_i^{\,2} + (y_i - y_0)^2}$$
$$q_i = \arctan\left(\frac{y_i - y_0}{x_i}\right)$$

In here, q_i is defined as $-p/2 \le q_i \le +p\,2$.

If the denominator is negative, depending on the sign of the numerator p has to be added or subtracted, so that q_i will be defined as $-p \le q_i \le +p$.

By elementary two-dimensional kinematics, the unit vector in the direction q_i is:

$$t_i = -\bar{i} \cdot \sin q_i + \bar{j} \cdot \cos q_i$$

so that:

$$v^{(4)} = S^{(4)} \cdot t_i \cdot R_i$$
$$= -wA^{(4)}R_i(\bar{i} \sin q_i - \bar{j} \cos q_i) \sin wt$$

The normal components of the velocity at the midpoint of the i^{th} segment (x_i, y_i) are:

$$v_i^{(2)} = -wA^{(2)} \sin a_i \sin wt$$
$$v_i^{(2)} = +wA^{(3)} \cos a_i \sin wt$$
$$v_i^{(2)} = +wA^{(4)} R_i \cdot \cdot (\sin q_i \sin a_i + \cos q_i \cos a_i) \sin wt$$

Defining:

$$n_i^{(m)} = \frac{v_i^{(m)}}{A^{(m)} w \sin wt}$$

then, consistent with the previously mentioned notation, the direction cosines for the three modes of motion are:

$$n_i^{(2)} = -\sin a_i$$
$$n_i^{(3)} = +\cos a_i$$
$$n_i^{(2)} = +\sin q_i \sin a_i + \cos q_i \cos a_i$$

A set of two coupled integral equations are applied by Frank at the midpoints of each of the N segments and is assumed that over an individual segment the complex source strength remains constant, although it varies from segment to segment. Then, the set of coupled integral equations becomes a set of $2N$ linear algebraic equations in the unknowns.

The hydrodynamic pressure $p^{(m)}$ along the cylinder is obtained from the velocity potential by means of the linearised equation of Bernoulli, where $p_a^{(m)}$ and $p_v^{(m)}$ are the hydrodynamic pressures in phase with the displacement and in phase with the velocity, respectively.
The potential as well as the pressure is a function of the oscillation frequency w.
The hydrodynamic force or moment per unit length on the cylinder, necessary to sustain the oscillations, is the integral of $p^{(m)} \cdot n^{(m)}$ over the submerged contour of the cross section C_0.
It is assumed that the pressure at the i^{th} midpoint is the mean pressure for the i^{th} segment, so that the integration reduces to summation, whence:

$$M^{(m)}(w) = 2\sum_{i=1}^{N} p_a^{(m)}(x_i, y_i, w) \cdot n_i^{(m)} \cdot |s_i|$$
$$N^{(m)}(w) = 2\sum_{i=1}^{N} p_v^{(m)}(x_i, y_i, w) \cdot n_i^{(m)} \cdot |s_i|$$

for the potential mass and damping forces or moments, respectively.

Frank's method is suitable for the computation of the potential mass and damping of symmetric 2-D shapes, in or below the surface of a fluid. This method has been incorporated in a lot of 2-D ship motion computer codes, all over the world. Starting from the keel point of the cross section, the input data of the off sets have to be read in an upward order. Then, the (outward) normal on the elements of the cross section will be defined to be positive in the direction of the fluid outside the cross section.

Easily, this method can be used to calculate the linear loads due to a potential fluid in an oscillating symmetrical tank too. Starting from the intersection of the free surface with the tank wall, the offsets of the tank have to be read in a downwards order, so in an opposite direction as has to be done for the cross sections of a ship. When doing this, the (inward) normal on the elements of the cross section of the tank will be defined to be positive in the direction of the fluid in the tank. Then, the calculated potential mass and damping delivers the in and out phase parts of the loads due to the moving liquid in the tank.
With this, the in and out phase parts of the 2-D excitation forces and moments about the origin in the water surface of the fluid in a rectangular tank are found with:

$$X_{2c} = w^2 M^{(2)} x_{2a}$$
$$X_{2s} = -wN^{(2)} x_{2a}$$
$$X_{3c} = w^2 M^{(3)} x_{3a}$$
$$X_{3s} = -wN^{(3)} x_{3a}$$
$$X_{4c} = w^2 M^{(4)} x_{4a} + + rg\left\{bh\left(s + \frac{h}{2}\right) + \frac{b^3}{12}\right\} x_{4a}$$
$$X_{4s} = -wN^{(4)} x_{4a}$$

This very simple approach can be carried out easily with many existing 2-D (and also 3-D) ship motions computer programs.
However, one should keep in mind that in the calculation routine of Frank, the angles a_i and q_i have to be defined well in all four quadrants.

2.3 Validations

Three different validations were performed to verify the validity of using Frank's pulsating source method for obtaining the moments caused by the motions of liquids in oscillating tanks.

Firstly, results of extensive model experiments on rectangular free surface anti-rolling tanks, carried out in the past by Van den Bosch and Vugts (1966), have been used.

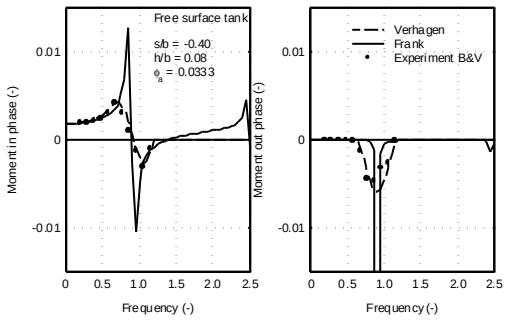

Figure 3 Roll Moments of a Free Surface Tank with Bottom below G

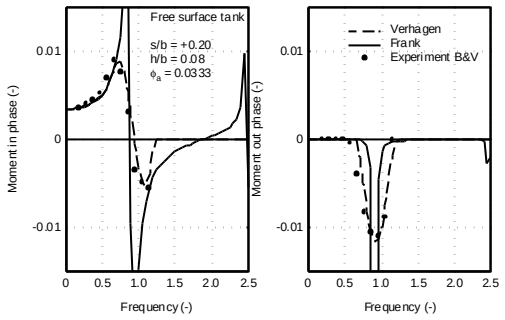

Figure 4 Roll Moments of a Free Surface Tank with Bottom above G

Figure 3 and Figure 4 show a few comparisons between calculated and measured in and out phase parts of the first harmonic of the roll moments for very small water depths in the tank. The comparisons are given here for one filling level $(h/b = 0.08)$ and one roll amplitude $(f_a = 0.0333 = 1.9^0)$. Two positions of the bottom with respect to the rotation point, i.e. the center of gravity G of the vessel, have been taken: 40 per cent of the tank width below the axis of rotation $(s/b = -0.40)$ and 20 per cent above it $(s/b = +0.20)$. The roll moment has been made non-dimensional by dividing this moment through $r\,g\,b^3$. The non-dimensional frequency parameter has been obtained by dividing the frequency through $\sqrt{g/b}$.
Outside the natural frequency area, the figure shows a good agreement between Frank's method and the experiments. But, for frequencies close to the natural frequency, a very poor prediction has been found. Because of the appearance of a hydraulic jump or a bore at these frequencies, the linearised equations are not valid anymore. The calculated phase lags between the roll moments and the roll motions have a step of 180 degrees at the natural frequency, while the calculated roll moment amplitudes go to infinity.
Because of a distinction between frequencies close to the natural frequency and frequencies far from it, the shallow water method of Verhagen and van

Wijngaarden shows a good prediction at all frequencies.

Secondly, forced roll oscillation experiments have been carried out with a 2-D model of a cargo tank of an LNG carrier. A sketch of this 1:25 model of the tank is given in Figure 5.

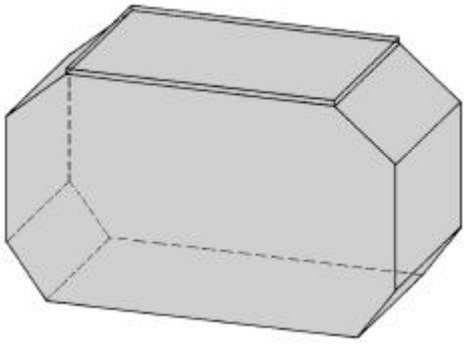

Figure 5 Model of an LNG Tank

At filling levels of 15, 45, 70, 90, 97.5 and 100 per cent of the depth of the tank, the exciting roll moments have been measured for a range of oscillation frequencies and one roll amplitude $\left(f_a = 0.10 = 5.7^0\right)$ of the tank. Because of the shape of this tank, a strong non-linear behaviour was expected at the lowest and highest free-surface levels.
Figure 6 through Figure 11 show the measured and predicted in-phase and out-of-phase parts of the first harmonic of the roll moments of the LNG tank as a function of the frequency.

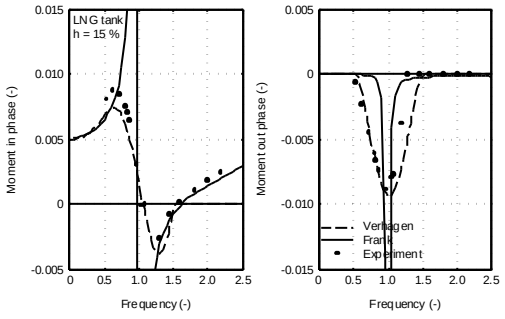

Figure 6 Roll Moments of an LNG Tank with 15 % Filling Level

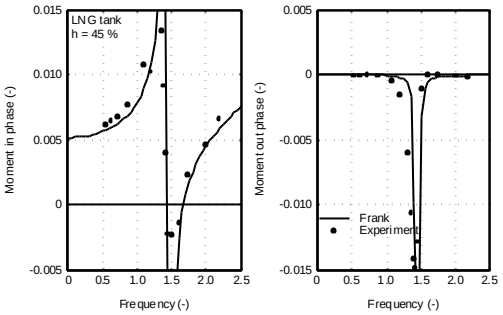

Figure 7 Roll Moments of an LNG Tank with 45 % Filling Level

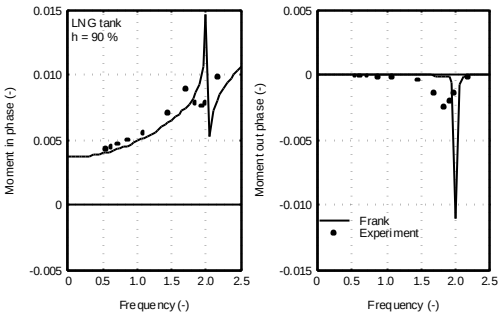

Figure 8 Roll Moments of an LNG Tank with 70 % Filling Level

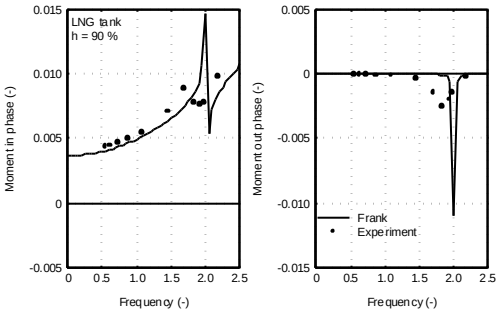

Figure 9 Roll Moments of an LNG Tank with 90 % Filling Level

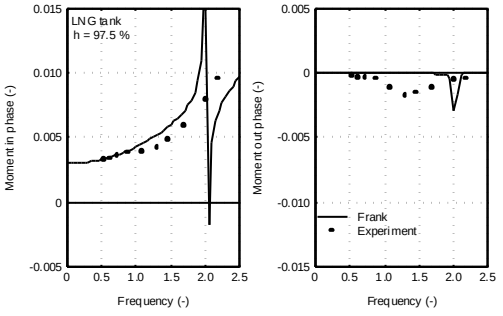

Figure 10 Roll Moments of an LNG Tank with 97.5 % Filling Level

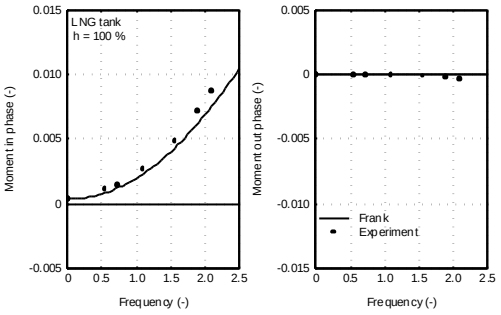

Figure 11 Roll Moments of an LNG Tank with 100 % Filling Level

The roll moment has been made non-dimensional by dividing this moment through $r\,g\,b^3$. The non-dimensional frequency parameter has been obtained by dividing the frequency through $\sqrt{g/b}$.
Except at the natural frequency of the fluid in the tank, a fairly good prediction has been found with Frank's method.
Again, the shallow water method of Verhagen and van Wijngaarden gives a good prediction for all frequencies at the lowest filling level of the tank.

Thirdly, a fully filled rectangular tank has been observed.
It is obvious that the ratio between the effective and the solified mass for sway or heave of the fluid in fully filled tanks is 1.0.
The ratio between the effective and the solified moments of inertia for roll of the fluid in a fully filled rectangular tank as a function of the aspect ratio h/b of the tank was given by Graham and Rodriques and published later by Silverman and Abramson (1966) as:

$$c_e = 1 - \frac{4}{1+\frac{h^2}{b^2}} + \frac{768}{\frac{p^5 h}{b}\left(1+\frac{h^2}{b^2}\right)} \cdot \sum_{n=0}^{\infty} \frac{\tanh\left\{(2n+1)\frac{ph}{2b}\right\}}{(2n+1)^5}$$

This expression had been obtained from results of space vehicle studies carried out by NASA. The contributions of frequencies higher than the first order are very small and can be neglected.
Calculations have been performed with the 2-D computer code SEAWAY of Journée (1996), that includes Frank's pulsating source method. Also, 3-D calculations have been carried out with the DELFRAC computer code of Pinkster (1996). The results are given in Figure 12.

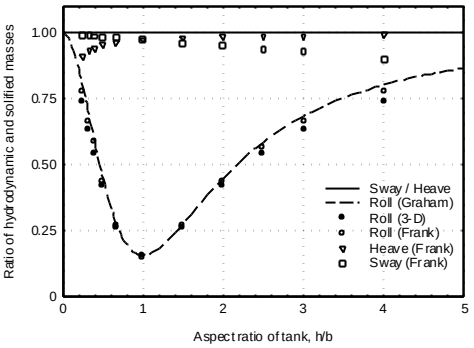

Figure 12 Moment of Inertia of a Fully Filled Tank

Figure 12 shows a fairly good agreement between these results. For small and large aspect ratios deviations can be expected, caused by the limited number of 16 line elements in SEAWAY or 30 panels in DELFRAC on the contour of half the cross section of the tank.

3 Ship Motions

To investigate the effect of free surface (liquid cargo) tanks on the roll motions of a ship, three tanks as given in Figure 5 were build in a 1:60 model of an LNG carrier. The body plan of this vessel is given in Figure 13.

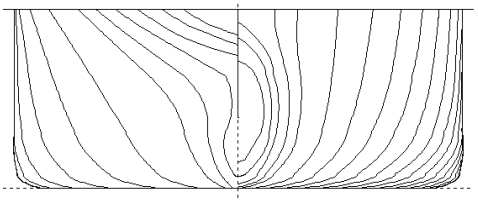

Figure 13 Body Plan of LNG Carrier

Static heel tests and roll decay tests in still water and roll motion measurements in regular beam waves with two different

wave amplitudes were performed at zero forward ship speed. These tests were carried out in Towing Tank I of the Ship Hydromechanics Laboratory of the Delft University of Technology with a length of 142 meter, a breadth of 4.22 meter and a water depth of 2.50 meter. The model was placed transversal in the towing tank at half the length of the tank and the spacing between the model and the tank walls was about 0.70 meter. The model was free to move in 6 degrees of freedom and the roll damping waves could propagate over a long distance before they were reflected to the model by the tank-ends.
The main dimensions of the ship are given in Table 1.

LNG Carrier			
Length bpp	L_{pp}	m	164.00
Breadth	B	m	32.24
Draught	d	m	12.60
Trim	t	m	0.00
Volume	∇	m^3	51680
Block coefficient	C_b	-	0.776
Length of bilge keels	l_{bk}	m	69.70
Height of bilge keels	h_{bk}	m	0.30
Gyradios for yaw	k_{zz}	m	45.43

Table 1 Main Dimensions of Ship

The length of each of the three cargo tanks was 13.45 meter and the distance of the bottom of the tanks above the ship's base line was 2.00 meter.
With the exception of these amidships cargo tanks 3, 5 and 7, all other cargo tanks are supposed to be filled up to 97.5 per cent of the inner tank height with a stowage factor of 1.00 ton/m^3. This was simulated in the experiments by solid ballast weights and an adaptation of the radius of inertia for roll of the ship.

For the cargo tanks 3, 5 and 7 three loading conditions have been chosen:

- Condition I: frozen liquids (45-45-45%)
  The three cargo tanks are equally filled up to 45% of the inner tank height with homogeneous frozen liquid cargo with a stowage factor of 1.00 ton/m^3, simulated by solid ballast weights.
- Condition II: liquids (45-45-45%)
  This condition is similar to condition I after melting the cargo, so the three tanks are partially filled with water.
- Condition III: liquids (45-70-15%)
  This condition is similar to condition II, but the filling levels of the three tanks are 45%, 70% and 15%, respectively.

The results of the static heel angle tests and the roll decay tests are given in Table 2.

Condition		I	II	III
∇	m^3	51680	51680	51360
KG	m	10.48	10.42	10.60
GM	m	2.75	2.81	2.62
GG'	m	0.00	1.69	1.59
k_{xx}	m	10.14	9.38	9.49
$T_{\phi\text{-meas.}}$	s	13.70	21.30	23.00
$T_{\phi\text{-calc.}}$	s		21.18	22.82

Table 2 Loading Conditions

The measured non-dimensional roll damping coefficients *k* are presented in Figure 14.

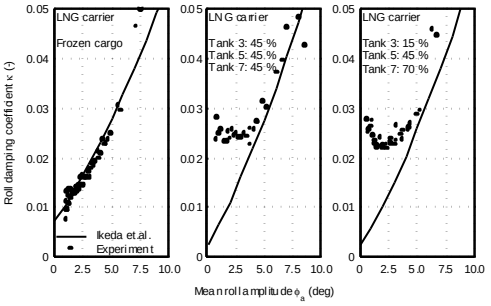

Figure 14 Roll Damping Coefficients

These data have been compared with predicted values obtained with the semi-empirical method of Ikeda.
For condition I, with frozen liquid cargo, a very good agreement has been found. For conditions II and III, with liquid cargo, the predicted roll damping coefficients are somewhat underestimated at smaller roll angle amplitudes. But at larger roll angle amplitudes, which are of interest in more dangerous circumstances, the figure shows a fairly good agreement.

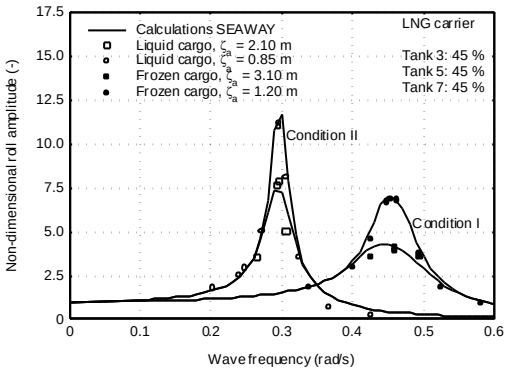

Figure 15 Roll Motions of LNG Carrier, Conditions I and II

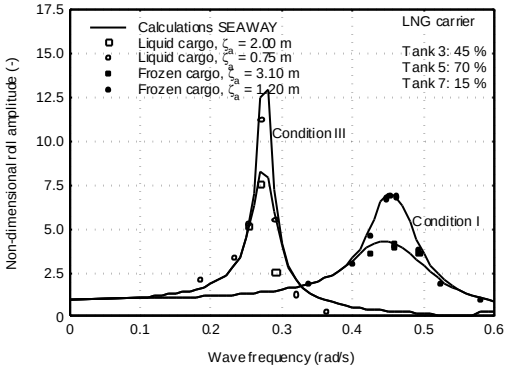

Figure 16 Roll Motions of LNG Carrier, Conditions I and III

Figure 15 and Figure 16 show a comparison of the measured and predicted roll amplitudes at two different wave amplitudes for each loading condition.

For loading condition I, the non-potential roll damping has been obtained by the method of Ikeda. The radius of inertia for roll of the ship's mass has been obtained from the measured natural roll period of 13.7 seconds and calculated hydromechanic coefficients. The figure shows a good agreement between experiments and predictions.

For the loading conditions II and III, the non-potential roll damping has been obtained by the method of Ikeda, Himeno and Tanaka (1978) too. The radius of inertia for roll of the ship's mass has been obtained from the radius of inertia of the ship with the frozen liquid cargo of condition I and a theoretical correction for melting this cargo. The deviating volume of liquid cargo in condition III has been accounted for too. The exciting roll moments due to liquid cargo have been obtained with Frank's method.

So, for the loading conditions II and III, the roll motions have been calculated without using any experimental data of these loading conditions. Table 2 shows a very good agreement between the predicted and the measured natural roll frequencies; the deviation is less than 1%. Nevertheless some overestimation at higher frequencies, Figure 15 and Figure 16 show a very good agreement between the predicted and the measured response amplitude operators for roll.

However, it may be noted that for the loading conditions II and III, the natural roll frequency of the ship is about half the lowest natural frequency of the fluid in the three cargo tanks. When these frequencies are close to each other, non-linear effects caused by the bore or the hydraulic jump at the surface of the fluid in the tanks will play a much more important role.

4 Conclusions

From the calculations and the experiments, the following conclusions can be drawn:

1. At very low filling levels of the tank, the method of Verhagen and van Wijngaarden predicts the exciting roll moments fairly good. Because this theory is given for shallow water only, the method fails for higher filling levels.
2. With the exception of frequencies near to the natural frequency of the fluid in the tank, the potential theory of Frank predicts the exciting roll moments fairly good for all filling levels of the tank.
3. An addition of these roll moments in the right hand side of the equation of motions of the ship, results in good predictions of the roll motions of the ship.
4. The non-linear roll damping of the ship plays an important role in these roll motions. Linearisation results in a

good prediction of the harmonic roll motions.

The pulsating source method of Frank, as included in many strip-theory ship motions computer programs, can be used easily to include the effect of non-viscous liquid cargo in ship motion calculations.
Also, 3-D calculation techniques for calculating potential mass and damping of ships can be used for this purpose.

5 References

Van den Bosch and Vugts (1966)
J.J. van den Bosch and J.H. Vugts, *Roll Damping by Free Surface Tanks*, Report 83-S, 1966, NSRC-TNO, Delft, The Netherlands.

Frank (1967)
W. Frank, *Oscillation of Cylinders in or below the Free Surface of Deep Fluids*, Report 2375, October 1967, NSRDC, Washington D.C., U.S.A.

Ikeda, Himeno and Tanaka (1978)
Y. Ikeda, Y. Himeno and N. Tanaka, *A Prediction Method for Ship Rolling*, Report 00405, December 1978, Department of Naval Architecture, University of Osaka Prefecture, Japan.

Journée (1996)
J.M.J. Journée, *The Behaviour of Ships in a Seaway*, Report 1049, May 1996, Ship Hydromechanics Laboratory, Delft University of Technology, The Netherlands.

Pinkster (1996)
J.A. Pinkster**,** *Hydrodynamic Aspects of Floating Offshore Structures*, Report 1050, May 1996, Ship Hydromechanics Laboratory, Delft University of Technology, The Netherlands.

Silverman and Abramson (1966)
S. Silverman and H.N. Abramson, *The Dynamic Behavior of Liquids in Moving Containers*, Edited by H.N. Abramson, Chapter 2: Lateral Sloshing in Moving Containers, Report NASA SP-106, 1966, Scientific and Technical Information Division, National Aeronautics and Space Administration, Washington D.C., USA.

Verhagen and van Wijngaarden (1965)
J.H.G. Verhagen and L. van Wijngaarden, *Non-linear Oscillations of Fluid in a Container*, Journal of Fluid Mechanics, 1965, Volume 22, Part 4, Pages 737-751.